

## **Supplementary information for**

### **SPNS2 exports sphingosine-1-phosphate and imports glucose**

**Cynthia Weigel<sup>1\*</sup>, Md Lokman Hossen<sup>2,6</sup>, Ryan D.R. Brown<sup>1,7</sup>, Can E. Senkal<sup>1</sup>, Christopher D. Green<sup>1</sup>, Jason Newton<sup>1,8</sup>, Sumit Saha<sup>1</sup>, Elisa N.D. Palladino<sup>1</sup>, Bin Ni<sup>3</sup>, Francesco S. Celi<sup>3,9</sup>, Xianjun Fang<sup>1</sup>, Frank D. Corwin<sup>4</sup>, Huanyu Z. Li<sup>5</sup>, David B. Sauer<sup>5</sup>, Prem P. Chapagain<sup>2</sup> & Sarah Spiegel<sup>1\*</sup>**

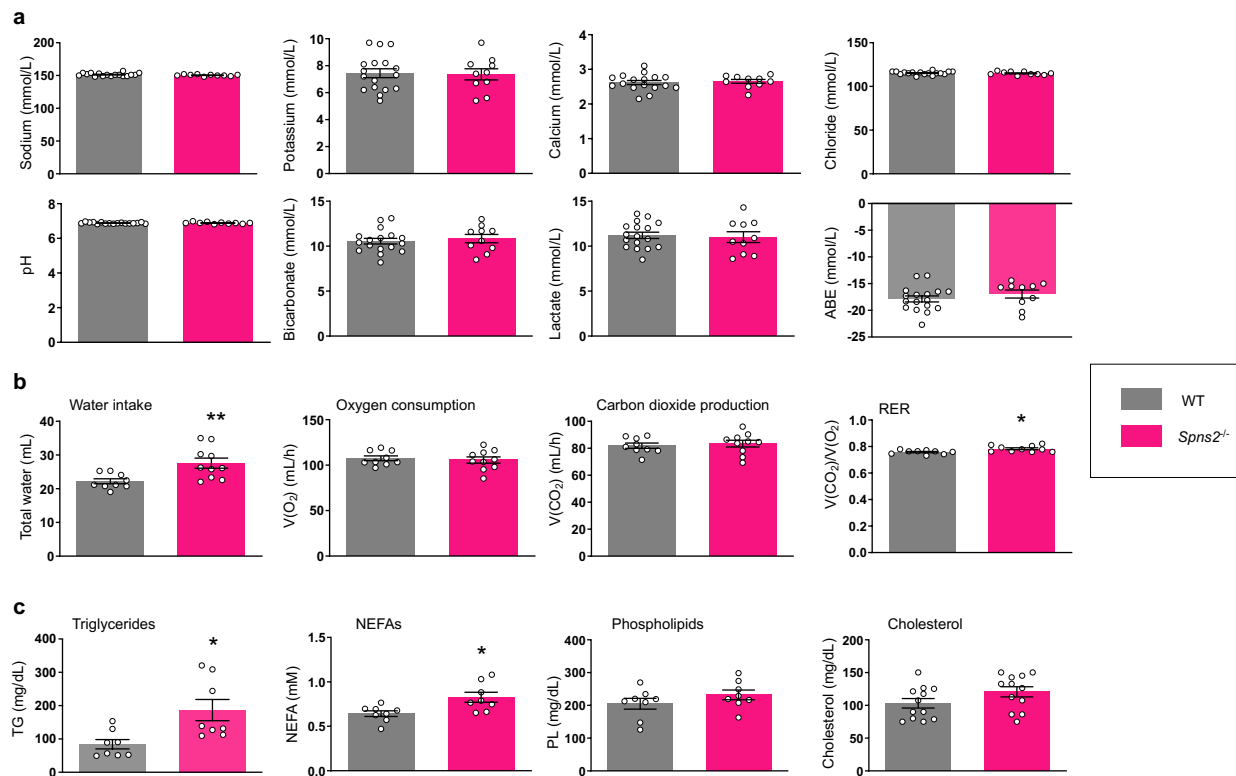
<sup>1</sup>Department of Cellular, Molecular and Genetic Medicine, Virginia Commonwealth University School of Medicine, Richmond, VA 23298, USA. <sup>2</sup>Department of Physics and Biomolecular Sciences Institute, Florida International University, Miami, Florida 33199, USA. <sup>3</sup>Department of Internal Medicine, Virginia Commonwealth University School of Medicine, Richmond, VA 23298, USA. <sup>4</sup>Department of Radiology, Virginia Commonwealth University School of Medicine, Richmond, VA 23298, USA. <sup>5</sup>Centre for Medicines Discovery, Nuffield Department of Medicine, University of Oxford; Oxford, UK.

Present addresses: <sup>6</sup>Department of Physics, University of Barishal, Kornokathi, Barishal-8254, Bangladesh; <sup>7</sup>School of Life Sciences, Keele University, Staffordshire, UK; <sup>8</sup>School of Life Sciences and Sustainability, Virginia Commonwealth University, Richmond, 23284; <sup>9</sup>Department of Medicine, UConn Health, University of Connecticut, Farmington, CT 06030.

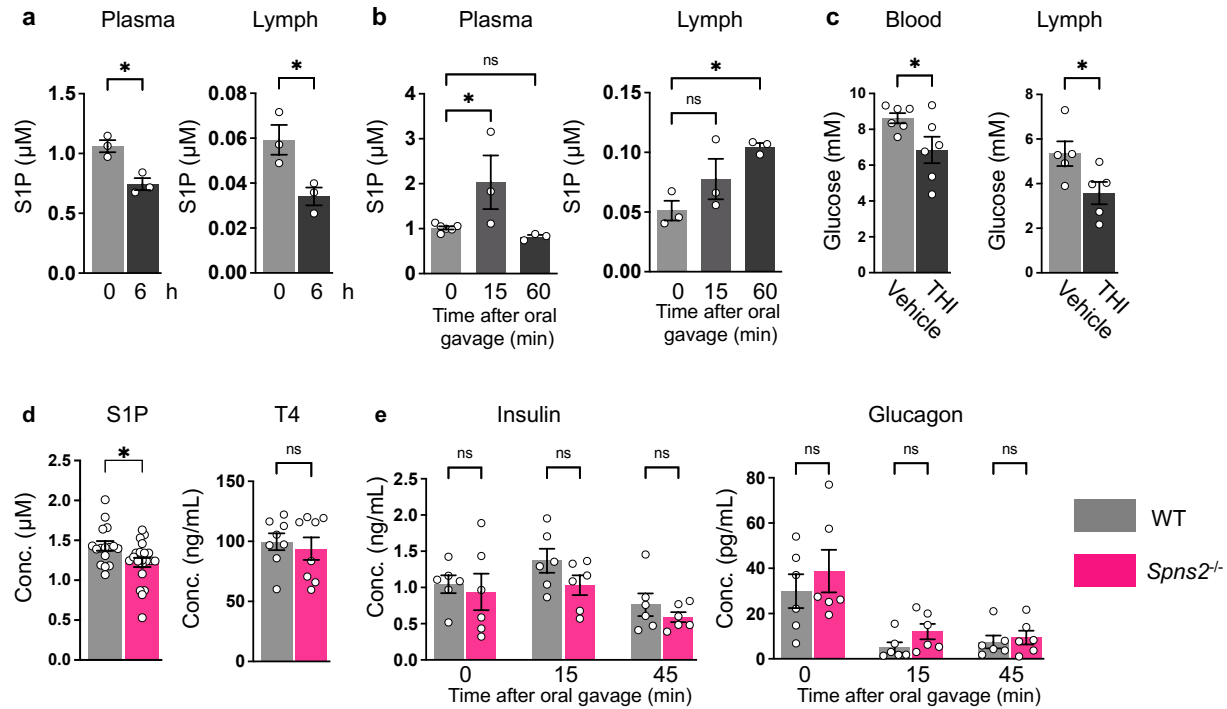
\*email: sarah.spiegel@vcuhealth.org; cynthia.weigel@vcuhealth.org



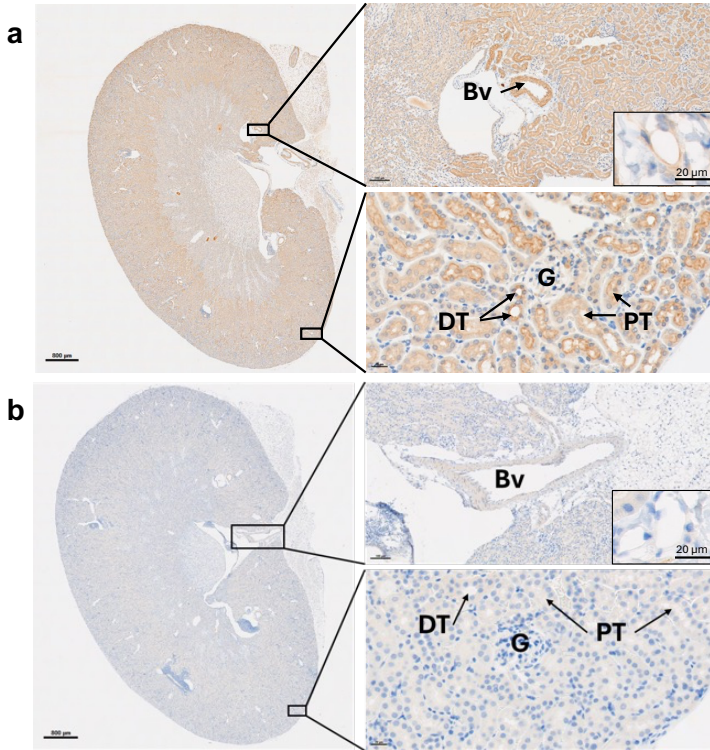
**Supplementary Figure 1. Evolutionary conservation profile of SPNS2 determined by ConSurf analysis.** Multiple-sequence alignment of 150 evolutionary conserved homologues of hSPNS2 across species showing the distribution of structural and functional residues in SPNS2 structure. According to the neural-network algorithm, 'e' signifies an exposed residue, 'b' is buried residues, 'f' is projected functional residues (notably conserved and exposed), while 's' designates projected structural residues (notably conserved and buried). The alignment is colored according to the ConSurf conservation scheme. 39.5% of all amino acids are predicted to be highly conserved, while 45% of those are potentially structural or functional, suggesting that SPNS2 functions are shared among members of the family.



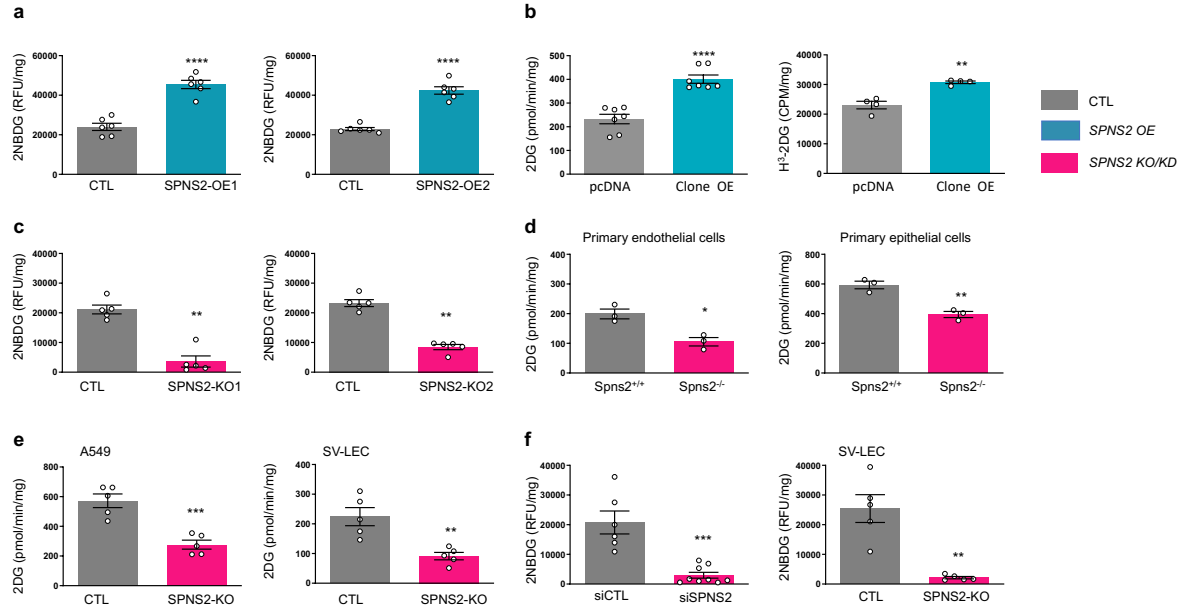
**Supplementary Figure 2. Deletion of SPNS2 in mice does not affect pH, blood ions, or respiratory exchange ratio.** **a** Blood analysis of sodium, potassium, calcium, chloride, pH, bicarbonate, lactate, and arterial base excess (ABE) from *Spns2*<sup>-/-</sup> and WT mice measured with a blood gas analyzer (n=17, 10; N=3). **b** Male *Spns2*<sup>-/-</sup> mice were individually housed for 7 days prior to metabolic chambers experiments. Water intake, O<sub>2</sub> consumption, CO<sub>2</sub> production and respiratory exchange ratio (RER) were measured with the PhenoMaster for 7 consecutive days (n=9,10; N=3). **c** **Dyslipidemia in *Spns2*<sup>-/-</sup> mice.** Plasma concentrations of triglycerides, cholesterol, phospholipids and non-esterified fatty acids (NEFAs) (n=8, 8), and cholesterol (n=12,12). Data are expressed as mean ± s.e.m. \*p < 0.05, \*\*p < 0.01, two-tailed unpaired t-test.



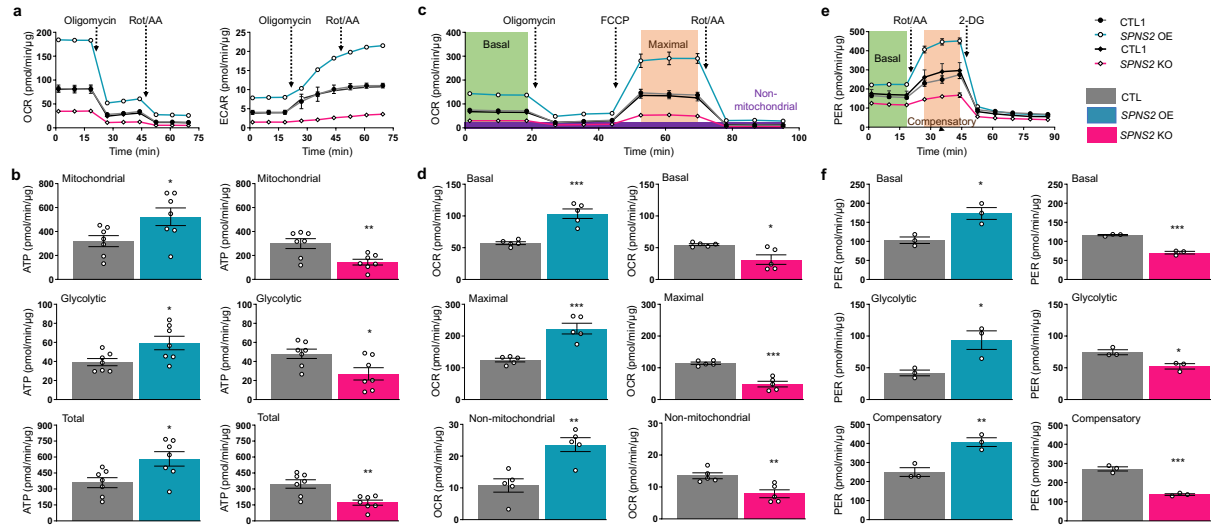
**Supplementary Figure 3. Blood glucose affects levels of lymph and plasma S1P.** **a** Levels of S1P were measured in plasma and lymph of WT mice before and after 6 hours fasting. (n=3). **b** Levels of S1P in plasma and lymph were measured before and 15 and 60 minutes after oral administration of glucose (2 g/kg body weight) to WT mice. (n=3). **c** WT mice were treated with 2-acetyl-4-tetrahydroxybutyl imidazole (THI) for 3 days (12.5 mg/kg/day) and glucose levels measured in blood (n=6, 6) and lymph (n=5, 5). Food deprivation for 6 hours decreased, and oral glucose increased plasma and lymph S1P levels. In addition, inhibiting S1P lyase with the specific inhibitor THI, which increases blood S1P<sup>1,2</sup>, decreased blood and lymph glucose levels, consistent with a previous report<sup>3</sup>. Of note after 6 hours fasting, *Spns2*<sup>-/-</sup> mice without increased intake of glucose from the diet cannot compensate for increased glucose excretion (Fig. 1e,o), which leads to a reduction in their blood glucose (time 0 in Fig. 1i). **(d,e) Deletion of SPNS2 has no apparent effect on levels of insulin or glucagon or the thyroid hormone thyroxine (T4).** **d** Plasma levels of S1P (n=16, 21), and T4 (n=8, 8) in WT and *Spns2*<sup>-/-</sup> fed mice. **e** Fasting plasma levels of insulin and glucagon before and 15 and 45 minutes after oral administration of glucose (2 g/kg body weight) to WT and *Spns2*<sup>-/-</sup> mice (n=6, 6, N=3). Data are means ± s.d. \*p < 0.05, ns, not significant. **(a, c, d)** two-tailed unpaired t-test. **(b)** One-way analysis of variance test followed by Dunnett's multiple comparisons test. **(e)** One-way analysis of variance test followed by Šidák's multiple comparisons test.



**Supplementary Figure 4. SPNS2 expression in kidney.** Representative immunohistochemical staining of SPNS2 in kidney (n=3). **a** The proximal and distal tubules are positive for SPNS2, whereas the glomerulus is very weakly stained. Positive stained endothelial cells of small vessels are depicted in the insert. Bv: Blood vessel, G: Glomerulus, DT: Distal tubule, PT: Proximal tubule. **b** There was no staining after pre-incubation with the blocking peptide control immunogen for SPNS2.

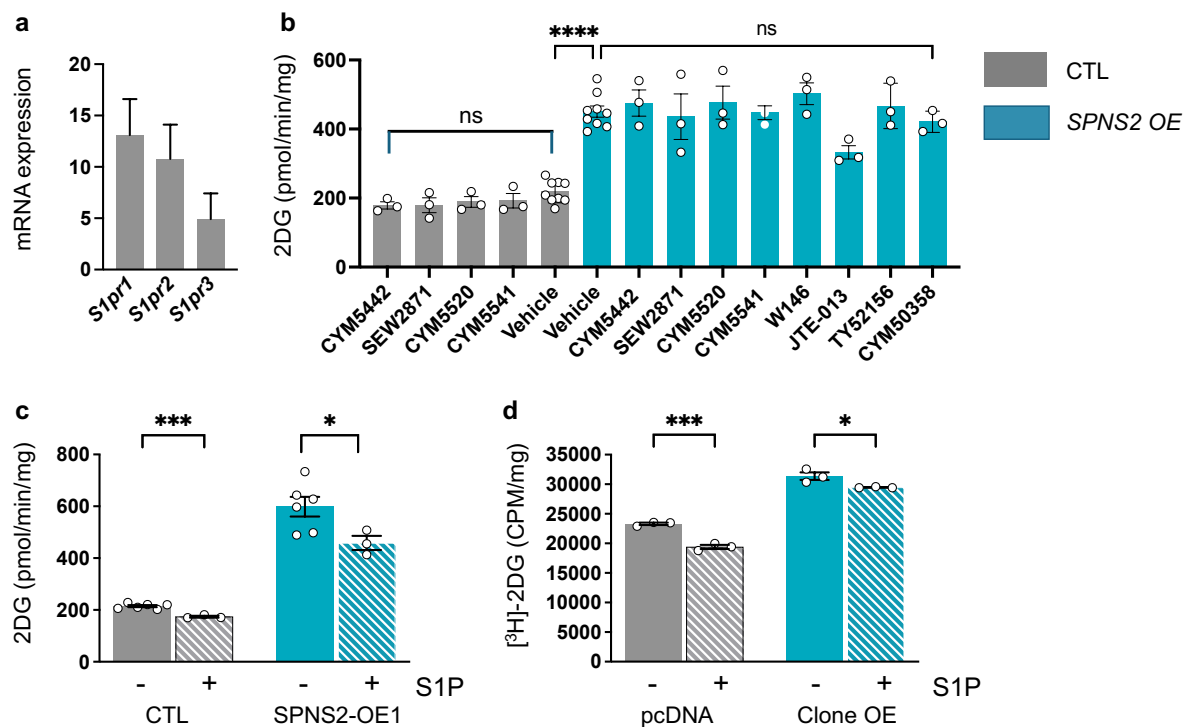


**Supplementary Figure 5. Overexpression of SPNS2 increases glucose uptake and its deletion decreases it in diverse cell types.** **a** 2NBD-glucose uptake was measured in *Spns2* stable overexpressing SVEC4-10 cell lines, SPNS2-OE1 (generated by CRISPR activation plasmids) and SPNS2-OE2 (generated by lentiviral activation particles) and in their corresponding controls. **b** 2DG or [<sup>3</sup>H] 2-Deoxy-D-glucose uptake was determined in SVEC4-10 cells stably transfected with *Spns2* plasmid (clone OE) or pcDNA control vector. **c** 2NBD-glucose uptake was measured in SPNS2-KO1 and SPNS2-KO2 cells (generated with CRISPR/Cas9 knock-out and homology-directed repair plasmids) and in their corresponding controls. **(d,e)** 2DG uptake was measured with the Glucose Uptake-Glo assay in **(d)** primary endothelial and epithelial cells isolated from *Spns2*<sup>-/-</sup> or *Spns2*<sup>+/+</sup> mice and in **(e)** A549 or SV-LEC *Spns2* knockout cells, generated by double nickase plasmids and their corresponding controls. **f** 2NBD glucose uptake was measured in SVEC4-10 cells transfected with siControl or siSPNS2 or in SPNS2 deleted lymph endothelial SV-LEC generated with double nickase plasmids (n=3-9, N=3). Data are means ± s.e.m. \*p < 0.05, \*\*p < 0.01, \*\*\*p < 0.001, \*\*\*\*p < 0.0001, two-tailed unpaired t-test.



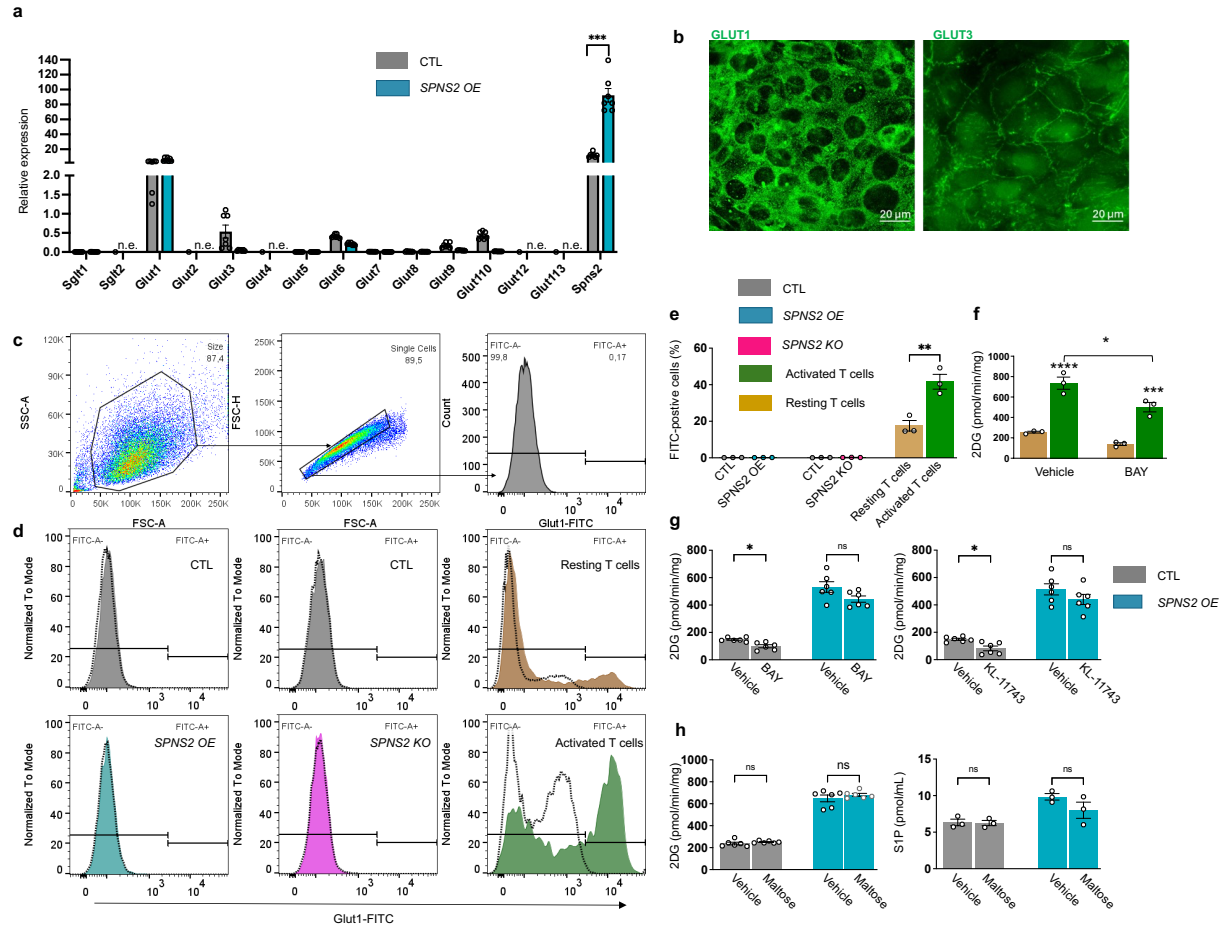
**Supplementary Figure 6. SPNS2 regulates ATP production, mitochondrial respiration, and glycolysis. (a, b)** Real-Time ATP rate measurement in Spns2 overexpressing (SPNS2-OE1) or Spns2 deleted cells (SPNS2-KO1) and their corresponding controls. **a** Oxygen consumption rate (OCR) and extracellular acidification rate (ECAR) were measured before and after the addition of Oligomycin, a complex V inhibitor, followed by Rotenone/Antimycin inhibitors of complex III and I, with the Seahorse XF Analyzer. **b** Mitochondrial, glycolytic, and total ATP rates were analyzed. **(c,d)** Mitochondrial stress test. **c** OCR was measured before and after the addition of Oligomycin, followed by the addition of carbonyl cyanide-p-trifluoromethoxyphenylhydrazone (FCCP), which collapses the inner membrane gradient, and Rotenone/Antimycin A using the Seahorse XF Analyzer. **d** Basal, maximal, and non-mitochondrial respiration rates were calculated. **(e,f)** Glycolytic rate analysis and proton efflux rates (PER) were calculated by simultaneous measurement of both OCR and ECAR before and after the addition of Rotenone/Antimycin inhibitors and after the addition of 2-deoxyglucose (2-DG). **f** Basal, glycolytic, and compensatory PER. Data are mean  $\pm$  s.e.m. of 3-7 independent experiments. \* $p < 0.05$ , \*\* $p < 0.01$ , \*\*\* $p < 0.001$ , two-tailed unpaired t-test.



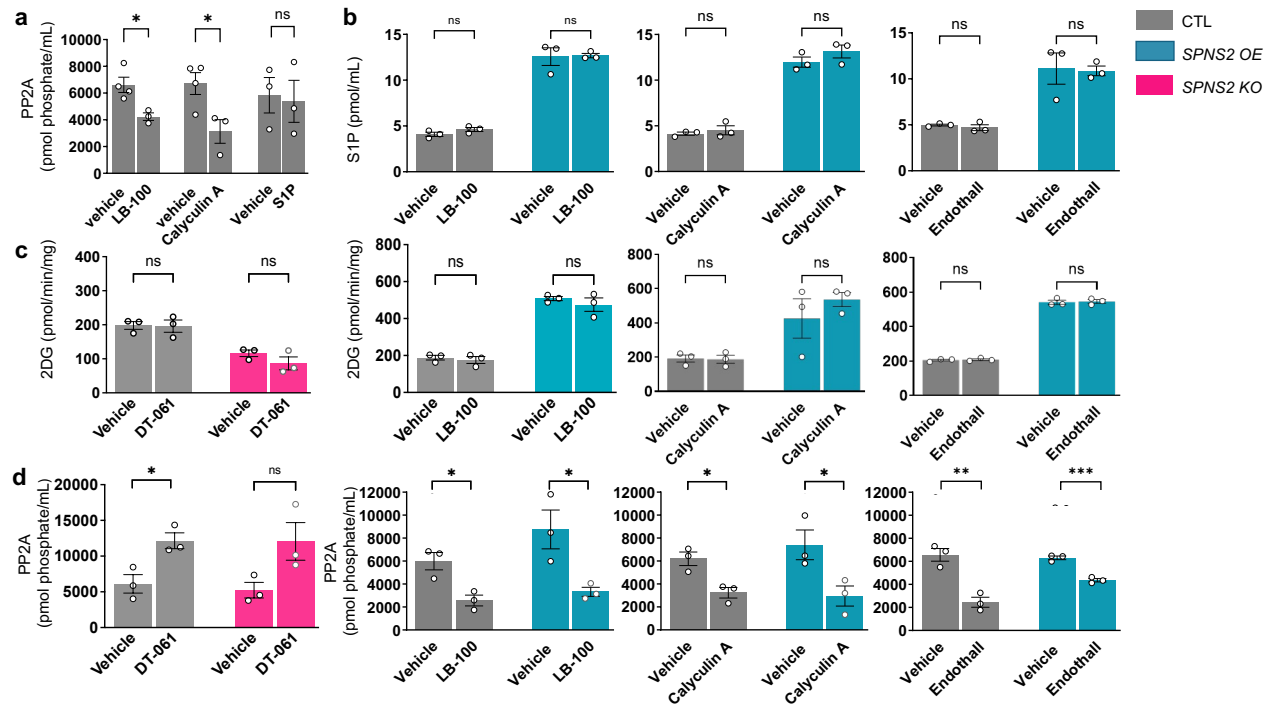


**Supplementary Figure 7. Lack of effect on glucose uptake by S1PR1-3 antagonists.** **a** mRNA expression of S1PR1–3 in SVEC4-10 cells normalized to reference genes *Hprt* and *Polr2a*. **b** *Spns2* overexpressing cells (SPNS2-OE1) and their controls (CTL1) cells were treated with 500 nM of S1PR agonists: CYM5442 (S1PR1), SEW2871 (S1PR1), CYM5520 (S1PR2) or CYM5541 (S1PR3), or with 3  $\mu$ M of the S1PR antagonists W146 (S1PR1), JTE-013 (S1PR2), TY52156 (S1PR3), or CYM50358 (S1PR4) as indicated, and glucose uptake determined. Data are mean  $\pm$  s.e.m (N=3). ns, not significant. There were no significant effects of agonists on vehicle-treated control cells or of antagonists on vehicle-treated overexpressing cells. While JTE-013, which has limited specificity for S1PR2, showed a trend toward reduced glucose uptake it is not statistically significant. One-way analysis of variance test followed by Dunnett's multiple comparisons test. **c** CTL and SPNS2-OE1 cells were treated without or with S1P (10  $\mu$ M) and 2DG uptake measured (n=3-6, N=3). **d** [<sup>3</sup>H] 2-Deoxy-D-glucose uptake was determined in SVEC4-10 cells stably transfected with *Spns2* plasmid (clone OE) or vector control treated without or with S1P (10  $\mu$ M) (n=3). Data are means  $\pm$  s.e.m. \*p < 0.05, \*\*\*p < 0.001, \*\*\*\*p < 0.0001, two-tailed unpaired t-test.

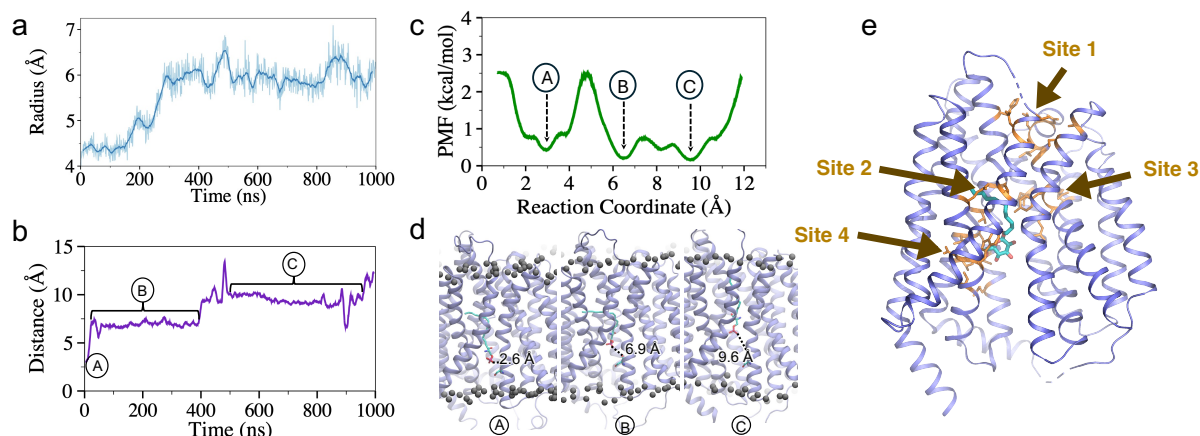




**Supplementary Figure 8. Increased glucose uptake in SPNS2 overexpressing cells is independent of the canonical glucose transporters GLUT1 and GLUT3 present on endothelial cells.** **a** Expression of glucose transporters, *Gluts* (*Slc2a1-13*) and sodium-coupled glucose transporters, *Sgl1* and *Sgl2* (*Slc5a1-Slc5a3*) in SPNS2 overexpressing cells (SPNS2-OE1) and their controls cells (CTL). \*\*\*p < 0.001, two-tailed unpaired t-test. n.e., not expressed. **b** SPNS2-OE1 cells stained with antibodies against GLUT1 or GLUT3 (green). Scale bar, 20  $\mu$ m. **c** Gating strategy of flow cytometric analysis of GLUT1 cell surface expression. **d** Cell surface abundance of GLUT1 was assessed in SPNS2-OE1, SPNS2-KO1, and their controls. The specificity of the GLUT1 antibody was confirmed in resting primary murine T lymphocytes that significantly upregulated GLUT1 on their cell surfaces upon activation with anti-CD3/CD28<sup>4</sup>. Representative histograms are shown with isotype control (dotted lines) and GLUT1 staining (filled). **e** Percentages of cell surface GLUT1-FITC positive cells were quantified. **f** Glucose uptake in naive and activated T cells treated with vehicle or the GLUT1 inhibitor BAY-876 (10 nM). **(g,h)** CTL and SPNS2-OE1 cells were treated without or with BAY-876 (2  $\mu$ M), KL-11743 (2  $\mu$ M), or maltose (500  $\mu$ M). Glucose uptake and S1P levels in the medium were measured as indicated. Data are mean  $\pm$  s.e.m. of 3-7 independent experiments. \*p < 0.05, \*\*p < 0.01, \*\*\*p < 0.001, \*\*\*\*p < 0.0001. One-way analysis of variance test followed by Tukey's or Sidak's multiple comparisons test.



**Supplementary Figure 9. SPNS2 regulates glucose uptake independently of PP2A.** **a** PP2A activity of human recombinant PP2A catalytic subunit was measured in the presence of vehicle, S1P (1  $\mu$ M), LB-100 (1  $\mu$ M), or Calyculin A (2 nM). **(b-d)** SPNS2-OE1, SPNS2-KO1 cells and their corresponding controls were treated with DT-061 (10  $\mu$ M), LB-100 (1  $\mu$ M), Calyculin (2 nM) or, Endothall (100 nM), as indicated. **b** S1P levels in the medium. **c** Glucose uptake. **d** PP2A holoenzyme was immunoprecipitated and its activity determined. (n=3). \*p < 0.05, \*\*p < 0.01, \*\*\*p < 0.001, two-tailed unpaired t-test.



**Supplementary Figure 10. The pathway of S1P translocation through SPNS2.** **a** To quantify expansion of the extracellular vestibule upon upward movement of S1P (shown in Fig. 4c), four Ca atoms of residues 124, 250, 337, and 363 were chosen in TM1, TM5, TM7, and TM8, respectively, and a best fit circle was drawn to represent the opening at that plane. During the simulation, as S1P moves upward, the initial radius of the opening increases and correlated with coordinated tilting, bending, and increased interhelical distances of TM5–TM8, TM1–TM7, and most prominently, TM7–TM8. In 3 independent runs, the radius increases by  $1.60 \pm 0.07$  fold. **b** Time evolution of the distance between the oxygen of the phosphate headgroup of S1P (O3 in the headgroup) and S232 (O in the backbone) of SPNS2 during the S1P translocation through SPNS2. **c** The Potential of Mean Force (PMF) profile along the reaction co-ordinate of S1P translocation. Distance in **b** was chosen as the reaction coordinate. The free-energy landscape of S1P translocation through SPNS2 shows three energy minima as indicated with A, B, and C. A set of representative SPNS2::S1P conformations at various minima is given in **d**, which indicate snapshots of the complex showing the positions of S1P relative to the reference S232 (O in the backbone) of SPNS2 corresponding to various free energy minima. **e** **Structure of SPNS2 (8QV6) determined with a bound dodecylmaltoside (DDM) molecule**<sup>5</sup>. The glucose coordinating residues of Sites 1 through 4, identified in molecular dynamics simulations, and DDM are highlighted in orange and cyan, respectively.

**Supplementary Table 1. Plasma membrane lipid composition.**

<b>Lipid Type</b>	<b># lipids in outer leaflet</b>	<b># lipids in inner leaflet</b>
POPC	102	30 (SPNS2::S1P) (IF) 29 (SPNS2::S1P::glucose) (IF) 30 (SPNS2::glucose) (OF)
POPE	20	92 (SPNS2::S1P) (IF) 93 (SPNS2::S1P::glucose) (IF) 92 (SPNS2::glucose) (OF)
PSM	57	12 (SPNS2::S1P) (IF) 15 (SPNS2::S1P::glucose) (IF) 12 (SPNS2::glucose) (OF)
POPS	10	40
PIP2	10	25
CHOL	50	55 (SPNS2::S1P) (IF) 53 (SPNS2::S1P::glucose) (IF) 55 (SPNS2::glucose) (OF)

**Supplementary Table 2. Simulation systems setup details.**

System in lipid bilayer	# K <sup>+</sup>	# Cl <sup>-</sup>	# H <sub>2</sub> O	Dimension (Å <sup>3</sup> )	Simulation time (ns)
Inward-facing SPNS2					
SPNS2::S1P	275	99	36907	127×127×117	200 ns (10 runs) 1000 ns (3 runs)
SPNS2::S1P::glucose	292	116	43208	127 x 127 x 130	600 ns (1 run) 1000 ns (2 runs)
Outward-facing SPNS2					
SPNS2::glucose	274	98	36797	127 x 127 x 117	600 ns (3 runs)

**Supplementary Table 3. List of primers used in this study**

Substitution		Sequence (5' to 3')	T <sub>m</sub> (°C)	recommended T <sub>a</sub> (°C)
T329A	forward	CTCCTTCGCCGCAGGGGCCCTGG	74	72
	Reverse	ACAGCCGACGTGGCCAGG	74	
E207A	forward	GGGCATCGGGGCGGCCAGCTACTC	76	72
	Reverse	ACCAGCCCCCGGGACAGG	76	
F410A	forward	CTCTGCCATCGCCATCTGCCTGATCTTCGTGGC	71	72
	Reverse	CCCAGCATGCCACGGCA	75	
E433A	forward	CTTCGTCGGGGCCACGCTGCTGT	69	68
	Reverse	ATACAGATATAGGCTCCTACGATGC	67	
R119A	forward	CTACCTGGACGCCTACACCGTGGCAGGC	63	64
	Reverse	TTGAGCACGTTGCCCAAG	63	
R200S	forward	GGTCCTGTCCTCAGGGCTGGTGG	63	64
	Reverse	AGCAGCCAGAAGTACTGC	65	
Y116A	forward	CGTGCTCAACGCCCTGGACAGGTAC	63	64
	Reverse	TTGCCCAAGCTGAGGATG	65	

**Supplementary Table 4. checklist for molecular dynamics simulations**

Reliability and reproducibility checklist for molecular dynamics simulations *All boxes must be marked YES by acceptance unless an N/A option is available	Yes	N/A	Response
<b>1. Convergence of simulations and analysis</b>			
1a. Is an evaluation presented in the text to show that the property being measured has equilibrated in the simulations ( <i>e.g.</i> time-course analysis)?	<input checked="" type="checkbox"/>		
1b. Then, is it described in the text how simulations are split into equilibration and production runs and how much data were analyzed from production runs?	<input checked="" type="checkbox"/>		
1c. Are there at least 3 simulations per simulation condition with statistical analysis?	<input checked="" type="checkbox"/>		Three replicas run for each system. Statistical analysis not needed.
1d. Is evidence provided in the text that the simulation results presented are independent of initial configuration?	<input checked="" type="checkbox"/>		
<b>2. Connection to experiments</b>			
2a. Are calculations provided that can connect to experiments ( <i>e.g.</i> loss or gain in function from	<input checked="" type="checkbox"/>		

mutagenesis, binding assays, NMR chemical shifts, J-couplings, SAXS curves, interaction distances or FRET distances, structure factors, diffusion coefficients, bulk modulus and other mechanical properties, etc.)?				
<b>3. Method choice</b>				
3a. Is it described in the text what force field and water model are used and why?		<input checked="" type="checkbox"/>		
3b. Do simulations contain membranes, membrane proteins, intrinsically disordered proteins, glycans, nucleic acids, polymers, or cryptic ligand binding?		<input checked="" type="checkbox"/>	<input type="checkbox"/>	Response not needed if N/A
	If 3b is <b>YES</b> , are enhanced sampling methods used?	<input type="checkbox"/>	<input checked="" type="checkbox"/>	Response not needed if N/A
	If enhanced sampling methods are used, are the convergence criteria clearly stated?	<input type="checkbox"/>		N/A
	If 3b is <b>YES</b> , is it explained in the text why or why not enhanced sampling methods are used?	<input checked="" type="checkbox"/>		
<b>4. Code and reproducibility</b>				
4a. Is a table provided describing the system setup, such as simulation box dimensions, total number of atoms, total number of water molecules, salt concentration, lipid composition (number of molecules and type)?		<input checked="" type="checkbox"/>		
4b. Is it described in the text what simulation and analysis software and which versions are used?		<input checked="" type="checkbox"/>		
4c. Are initial coordinate and simulation input files and a coordinate file of the final output provided as supplementary files or in a public repository?		<input checked="" type="checkbox"/>		
4d. Is there custom code or custom force field parameters?		<input type="checkbox"/>	<input checked="" type="checkbox"/>	Response not needed if N/A
	If <b>YES</b> , are they provided as supplementary profiles or in a public repository?	<input type="checkbox"/>	N/A	

## REFERENCES

- Schwab, S. R. *et al.* Lymphocyte sequestration through S1P lyase inhibition and disruption of S1P gradients. *Science* **309**, 1735-1739 (2005).
- Weigel, C. *et al.* S1P lyase inhibition protects against sepsis by promoting disease tolerance via the S1P/S1PR3 axis. *EBioMedicine* **58**, 102898 (2020).
- Qu, J. *et al.* Dendrobium Officinale Polysaccharide Attenuates Insulin Resistance and Abnormal Lipid Metabolism in Obese Mice. *Front Pharmacol* **12**, 659626 (2021).
- Macintyre, A. N. *et al.* The glucose transporter Glut1 is selectively essential for CD4 T cell activation and effector function. *Cell Metab* **20**, 61-72 (2014).
- Li, H. Z. *et al.* Transport and inhibition of the sphingosine-1-phosphate exporter SPNS2. *Nat Commun* **16**, 721 (2025).